Front. Phys. China, 2010, 5(4): 380–386
DOI 10.1007/s11467-010-0134-3

MINI-REVIEW ARTICLE

Understanding formation of molecular rotor array on Au(111) surface

Shi-xuan DU (杜世萱), **Ye-liang WANG** (王业亮), **Qi LIU** (刘奇), **Hai-gang ZHANG** (张海刚), **Hai-ming GUO** (郭海明), **Hong-jun GAO** (高鸿钧)†

Institute of Physics, Chinese Academy of Sciences, Beijing 100190, China
E-mail: †hjgao@aphy.iphy.ac.cn

Received June 29, 2010; accepted July 20, 2010

The motion of single molecules on surfaces plays an important role in nanoscale engineering and bottom-up construction of complex devices at single molecular scale. In this article, we review the recent progress on single molecular rotors self-assembled on Au(111) surfaces. We focus on the motion of single phthalocyanine molecules on the reconstructed Au(111) surface based on the most recent results obtained by scanning tunneling microscopy (STM). An ordered array of single molecular rotors with large scale is self-assembled on Au(111) surface. Combined with first principle calculations, the mechanism of the surface-supported molecular rotor is investigated. Based on these results, phthalocyanine molecules on Au (111) are a promising candidate system for the development of adaptive molecular device structures.

Keywords molecular rotors, scanning tunneling microscopy (STM), nanodevices

PACS numbers 85.85.+j, 63.20.dk, 68.37.Ef, 82.37.Gk

Contents

1 Introduction

Molecules are important building blocks for bottom-up fabrication of functional nanostructures. Low-dimensional molecular systems with intriguing physical properties have potential applications in fabricating nanodevices and nanomachines [1, 2]. The significant advantage of molecules lies in the well-developed molecular synthesis techniques which can produce various molecular structures with different properties [3–5]. By using suitable molecules and surfaces, ordered nanostructures can be easily constructed on surfaces [6–16]. Based on these characteristics, molecules are undoubtedly the most attractive candidates for the fabrication of nanodevices with integrated functions.

Molecular rotor is a type of a molecular machine that can rotate with respect to their surrounding environments [17, 18]. Based on their characteristic working principles, the driving force of molecular rotors can be heat [16, 19], photonics [20–23], electricity [24, 25], and chemical reactions [26]. At the molecular level, electrical driving of molecular rotors can also be realized by electron tunneling [27, 28]. Molecular rotors at solid surfaces have advantages of accessibility by using external fields [29, 30] and easy identification by surface analysis methods [31–33].

Scanning tunneling microscopy (STM) has the ability to study individual molecule at surfaces with atomic-scale precision, and therefore has helped scientists in revealing many interesting physics in surface science, including electron transport [10, 34, 35], spin-flip excitations [36, 37], vibrational excitations [38] and mechanical motions [16, 39, 40]. In addition, the STM tip can be used as a mechanical tool for manipulating atomic and molecular events not only on ensemble-averaged populations of species but also on single functional group of the chemical entities [41–46]. Therefore, STM could pro-

vide a unique tool to investigate the dynamic behavior in real time and mechanism of molecular rotors at the single molecular level.

In this paper, we focus on several thermally driven molecular motors based on metal phthalocyanine molecules at Au(111) surfaces. Large-scale ordered arrays of single molecular rotors are self-assembled on the Au(111) surfaces. The motion mechanism of a single molecular rotor is investigated. STM experiments and first-principle calculations reveal that gold adatoms were introduced on the Au(111) surface. An off-center rotation axis is formed by a chemical bonding between a nitrogen atom of phthalocyanine and a gold adatom on the surface, which gives the molecule a well-defined contact while rotating. A fixed rotation axis off center is an important step towards the eventual fabrication of molecular rotors or generators. It is found out that the motion of the molecular rotor can be manipulated by changing either the molecular structure or the STM tunneling current. An STM tip is also used to manipulate a nearby molecule to block the single molecular rotor, and an artificial 'gear wheel' structure has been successfully achieved by using two coupled rotating molecules. These results provide a fundamental understanding of molecular rotors.

2 Array of molecular rotors at the Au(111) surface

It is well known that the Au(111) surface can form a unique 22 $\times\sqrt{3}$ reconstruction after annealing at about 800 K. The top-layer atoms are laterally compressed along the [0 1–1] direction to fit 23 atoms into a length only large enough for 22 atoms in the bulk. Figure 1(a) shows the typical herringbone reconstructions observed by STM. The top layer consists of atoms in alternating face-centered cubic (FCC) and hexagonal close-packed (HCP) domains [Fig. 1(a)]. Atoms within the transition region between the FCC and HCP domains appear as bright discommensuration lines in our STM image [ridge in Fig. 1(a)]. Due to the threefold symmetry of the Au(111) surface, three rotational domains exist, and the transition from one domain to another takes place via correlated bending of the discommensuration lines by $\pm$ 120°. The corner of the lines is marked as elbow sites in Fig. 1(a). The width of the FCC region is approximately 50% larger than that of the HCP region [47, 48].

Recently, researchers deposited tetra-*tert*-butyl zinc phthalocyanine ((t-Bu)$_4$ZnPc) molecules [Fig. 1(b)] on the reconstructed Au(111) surface [16]. The molecule looks like a windmill with four protruding vanes surrounding an axis. It was found that the molecules adsorbed on each elbow site of the reconstructed Au(111) surface, self-assembled into a well-defined molecular array [Fig. 1(c)]. Fig. 1(d) shows the detailed configuration of the molecules. Each molecule shows a folding-fan structure, which is different from the molecular configuration shown in Fig. 1(b). The folding-fan structures at two different elbow sites show different features due to the modulation by corrugation ridges. Further investigation found that each folding-fan structure corresponds to one molecule which was rotating at the elbow site. Gold adatoms [49, 50], served as the stable contact of the molecules to the surface, provide a stationary rotating axis for the molecular rotor. This axis is formed by a chemical bond between a nitrogen atom of the molecule and a gold adatom on the surface, which gives them a well-defined contact while the molecules can have rotation-favourable configurations. These single-molecular rotors form large-scale ordered arrays due to the regular reconstruction of the Au(111) surface. Both the stationary axis and the self-assemble ability of the molecular rotors provide potential application possibility for the development of molecular nanodevices.

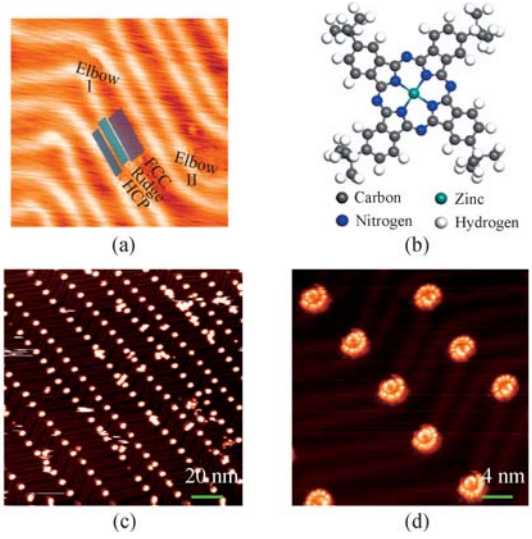

Fig. 1 (t-Bu)$_4$ZnPc on Au(111). **(a)** STM image of a reconstructed clean Au(111), in which four special regions with different arrangements of surface atoms are marked; **(b)** Structure of a (t-Bu)$_4$ZnPc molecule; **(c)** STM image of a large-scale ordered array of single (t-Bu)$_4$ZnPc molecular rotors on a reconstructed Au(111) surface. **(d)** High-resolution STM image of single molecular rotors showing a "folding-fan" structure at elbow sites. (Taken at 78 K by 0.07 nA, −1.3 V). Reprinted with permission from Ref. [16].

3 Single molecular rotors at Au(111) surface

3.1 (t-Bu)$_4$ZnPc/Au(111)

At very low coverage, (t-Bu)$_4$ZnPc molecules can be found on different regions of the reconstructed Au(111) surface, elbow, ridge, FCC and HCP. The molecules located at the elbow sites show folding-fan structures [Fig. 2(c)]. The STM images of the molecules located in FCC,

HCP regions and on the ridges show "flower" features [Fig. 2(a), (b) and (d), respectively]. More specifically, STM images of molecules on FCC and HCP regions are composed of two concentric cirques: twelve bright lobes form the outer torus, just like twelve "petals", while the inner torus has no obvious divisions. The STM image of the molecular rotors on the ridges is composed of an outer torus by twelve bright lobes, but with two inner elliptic protrusions. Both the folding-fan and flower features can only be seen at temperature of 78 K. The STM image of a single molecule only shows a four-lobe structure at 5 K.

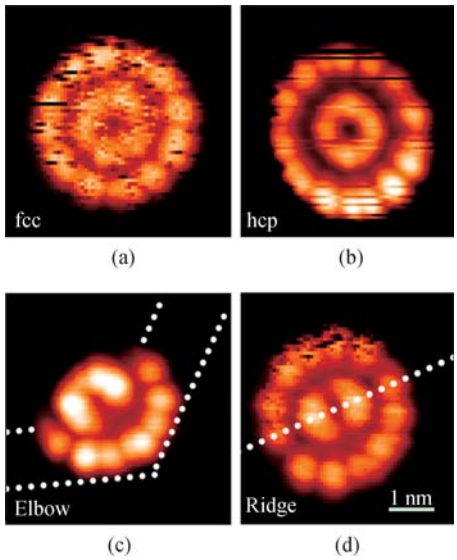

Fig. 2 High-resolution STM images of single molecular rotors formed by (t-Bu)$_4$ZnPc molecules at different substrate regions, FCC **(a)**, HCP **(b)**, elbow **(c)** and ridge **(d)**. (taken at 78 K, 0.07 nA, −1.3 V).

In order to demonstrate that the "folding-fan" structure is caused by molecular motion with respect to the substrate, the authors monitored the tunneling current versus time by locating the STM tip at a fixed point on a "folding-fan" structure [Fig. 3(a)]. They applied a constant bias voltage of –1.8 V to the sample, and recorded the tunneling current as a function of time. Figure 3(b) shows the recorded tunneling current within a time interval of 80 ms. The amplitude of the tunneling current oscillates frequently between 0 and 5 nA. The oscillation provides direct evidence that the "folding-fan" structure is really due to rapid molecular motion.

However, question remains that how many molecules there are in one "folding-fan" structure. The authors proved that this structure involved only one (t-Bu)$_4$ZnPc molecule. In fact, a stationary single (t-Bu)$_4$ZnPc molecule, whose STM image should be composed of four lobes, cannot be observed at 78 K. Only folding-fan, flower-like structures, and different aggregates of dimers, trimers, tetramers, and larger clusters of (t-Bu)$_4$ZnPc molecules can be observed at 78 K using STM. This indicates that a single molecule is not stationary on the surface at this temperature. Besides, the molecule which shows a four-lobe structure changed to a "folding-fan" structure when shifting its neighboring molecules with an STM tip [marked by the white arrows in Fig. 4(a) and (b)]. It was clear that the molecule began moving when its neighbor was moved away. And it remained stationary when it was attached by the neighboring molecule.

In another experiment, a sequence of images showed that such kind of move-stop process is reversible. The authors observed a single molecule [marked with white arrow in Fig. 4(c)–(f)] bounced between the molecular dimer at bottom-right and a "flower" like molecule at up-left. The arrowed molecule can block the rotating molecule (up-left) by forming a new molecular dimer [Fig. 4(d)], and then the molecule begins rotating when detaching the arrowed molecule by the STM tip [Fig. 4(e)]. Reversibly, it stops rotating if it is attached again by the arrowed molecule [Fig. 4(f)]. These manipulations also clearly demonstrate that the folding-fan and flower-like structures are due to the rotation of a single (t-Bu)$_4$ZnPc molecule on the reconstructed Au(111) surface.

The existence of a rotation axis is the prerequisite for rotation; otherwise, a lateral diffusion of (t-Bu)$_4$ZnPc molecules along the surface would be hard to block at

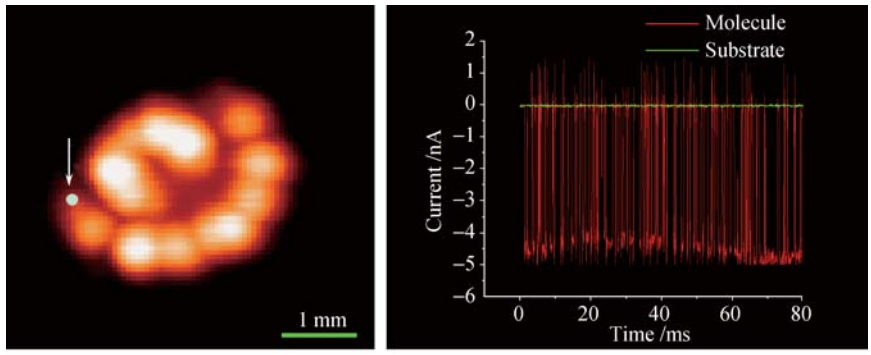

Fig. 3 **(a)** A high-resolution STM image of single (t-Bu)$_4$ZnPc molecular rotor showing a "folding-fan" structure (0.05 nA, –2 V). **(b)** *I*–*t* spectra measured on the molecular rotor (*red curve*) and the substrate (*green curve*), and the *I*–*t* spectra of the molecule was measured at the position indicated by the arrow in (a). Reprinted with permission from Ref. [16].

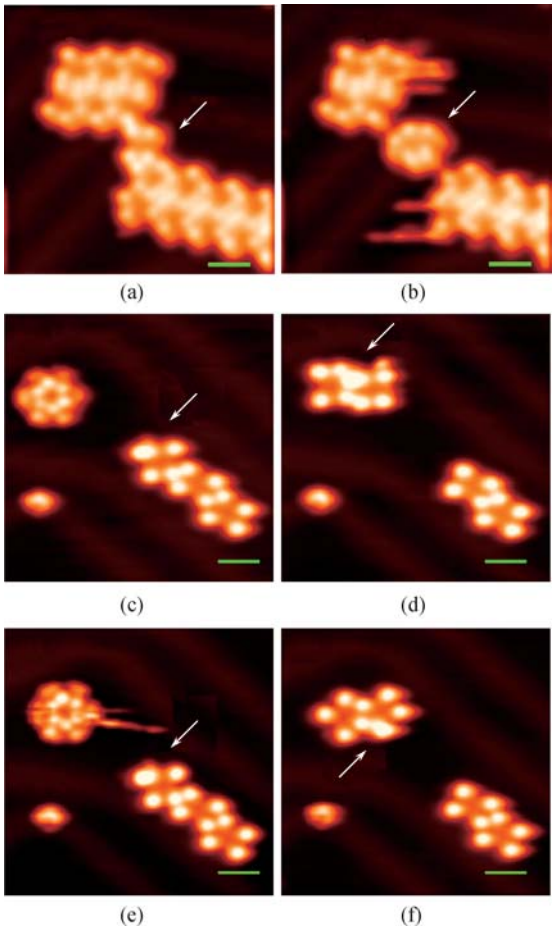

Fig. 4 Sequences of STM images showing the manipulation of (t-Bu)$_4$ZnPc molecular rotor on Au(111) surface by STM tip. **(a)** The molecule indicated by an arrow remains stationary, due to attaching by the two adjacent molecular clusters formed by same molecules; **(b)** The same molecule in (a) rotates while it is released when the adjacent molecules were moved by the STM tip; **(c)**–**(f)** show a repeatable process in which the molecule indicated by an arrow bounced between a rotating molecule (up-left) and a molecular dimer (bottom-right), switching the rotor (up-left) between rotation and stationary.

increasing temperatures. The rotation axis cannot be at the position of the *tert*-butyl groups which appear as bright protrusions in STM measurements. Combined further STM observations with the first-principle calculations, the researchers revealed that the rotation axis is the bond between a trapped gold adatom at the surface and the nitrogen atom in the molecule. By manipulating with an STM tip, one molecule with the folding-fan structure located at the elbow site [Fig. 5(a)] was removed. A small bright spot at the center position of the molecular rotor was observed [16], as shown in Fig. 5(b). This bright spot, observed after the removal of a single molecule, is proposed as a gold adatom. Gold adatoms on the reconstructed gold surface are stable and prefer to adsorb at the elbow sites at 78 K [49]. It can enhance the interaction between the adsorbed molecule and the surface, thus forming a potential energy well that prevents lateral diffusion of the molecule on the surface.

The existence of gold adatom is further proved based on the first-principle calculations. Figure 5(c) and (d) are the top and side views of the optimized configuration for a single (t-Bu)$_4$ZnPc molecule adsorbed on a gold adatom, respectively. The calculation results show that the distance between the zinc atom and its nearest-neighboring gold atom is 4.60 Å; the distance between the nitrogen (colored in yellow) and the gold adatom is 2.25 Å; the adsorption energy of this configuration is 804 meV. In contrast, for a single (t-Bu)$_4$ZnPc molecule adsorbed directly on Au(111), the distance between the zinc atom and its nearest-neighbor gold atom is 4.35 Å [16]; the distance between the nitrogen atom and its nearest-neighbor gold atom is 4.40 Å; the adsorption energy of this configuration is only 219 meV, which is much smaller than the one with gold adatom. Obviously, the gold adatom significantly enhances the molecular bonding, which is most likely due to the surface dipole originating from smeared-out electron charge at the position of the adatom [50]. Thus, the strong chemical bond between nitrogen and the gold adatom prevents lateral molecular diffusion on Au(111) surface. In particular, it offers a fixed off-center axis for the rotation of a single (t-Bu)$_4$ZnPc molecule at 78 K. The model is in good agreement with the experimental observations. The distance between the rotor center and the bright lobes on the outer torus is 1.3 $\sim$ 1.4 nm according to the STM image, which is in agreement with the distance between the nitrogen atom and the *tert*-butyl groups (1.10 $\pm$ 0.05 nm), considering that the rotation center is the

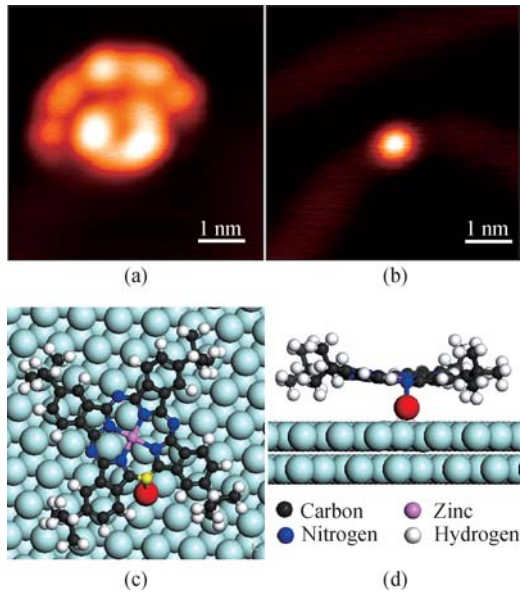

Fig. 5 **(a)** STM image of a (t-Bu)$_4$ZnPc molecular rotor located at the elbow position of the substrate. **(b)** STM image after STM manipulation, bright spot indicates a gold adatom after removing the attached molecule. **(c)** and **(d)** Top view and side view of the optimized configuration of a (t-Bu)$_4$ZnPc molecule adsorbed on an Au(111) surface via a gold adatom (*colored by red*), respectively. The adatom acts as an off-center rotation axis for molecular rotation.

gold adatom which is not exactly under the nitrogen atom.

For a single (t-Bu)$_4$ZnPc molecular rotor on a flat Au(111) surface, the calculations found that there are twelve stable adsorption configurations, which are 30 degrees apart from each other and can be interpreted as intermediate states. The differences in adsorption energies between these stable configurations are only tens of meV. The molecule switches between them with high frequency under thermal excitation. Since four *tert*-butyl groups are imaged as the bright lobes in STM measurements [see Fig. 6(a)], the ensuing STM image is the "flower"-like structure. The proposed STM image for 360° rotation is in good agreement with the "flower"-like structures observed in the experiments [Fig. 6(c)]. The HCP and FCC regions of the surface have similar symmetry with respect to the rotation axis; thus, the molecular rotors in the two regions have almost identical STM images. The rotation of single (t-Bu)$_4$ZnPc molecule at the elbow sites is interpreted based on the model for the rotation in the FCC region. The corrugation of the ridges limited the rotation of the molecule at the elbow sites within an angle of 120° due to the bending of the ridges, which leads to the "folding-fan"-like structure. The proposed STM image for 120° rotation is in good agreement with the experimental STM image of a single molecule at the elbow site [Fig. 6(b)]. Here, the variation of the position of surface atoms leads to a redistribution of potential barriers for molecular rotation.

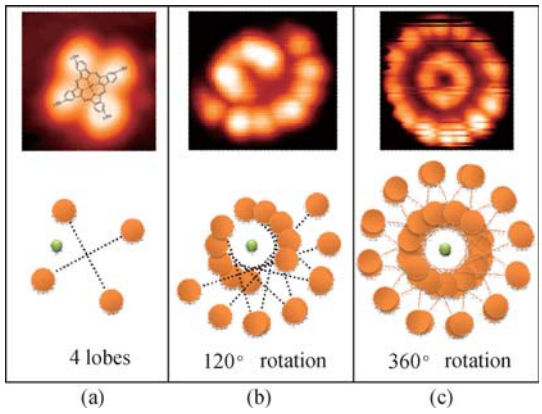

Fig. 6 STM images and schematic drawing of a single (t-Bu)$_4$ZnPc molecule on an Au(111) surface. **(a)** Stationary molecule show a 4-lobe structure, the image is taken at 5 K. **(b)** and **(c)** rotors with rotation angles of 120° and 360° with the appearance of folding-fan, and flower, respectively. These two images are obtained at 78 K. The orange solid circles depict the bright lobes for stationary single molecules, and the light-green circle represents the rotation center (gold adatom).

3.2 FePc and ZnPc on Au(111)

The researchers further revealed that such kind of a molecular rotor exists widely for phthalocyanine molecules [51]. By modifying either the central metal atoms or the functional groups linked to the planar molecular backbones, different kinds of molecular rotors with different diameter and rotation-favorable configurations are shown in Fig. 7. Three different folding-fan structures constituted of (t-Bu)$_4$ZnPc, ZnPc and FePc molecules are demonstrated at 78 K, respectively. When the temperature decreased to 5 K, the molecules show four bright spots, cross with a dark center for (t-Bu)$_4$ZnPc and ZnPc, and cross with a bright center for FePc. It is clear that all of them have similar rotating mechanisms. However, due to tert-butyl groups, (t-Bu)$_4$ZnPc has a larger rotation diameter than ZnPc and FePc [Fig. 7(a)]. For the FePc molecule, the central iron atom of FePc shows a bright spot in the STM image [Fig. 7(c)]. Thus, the center of its folding-fan structure shows a low contrast compared with ZnPc which shows a dark dip in the molecular center [Fig. 7(b)].

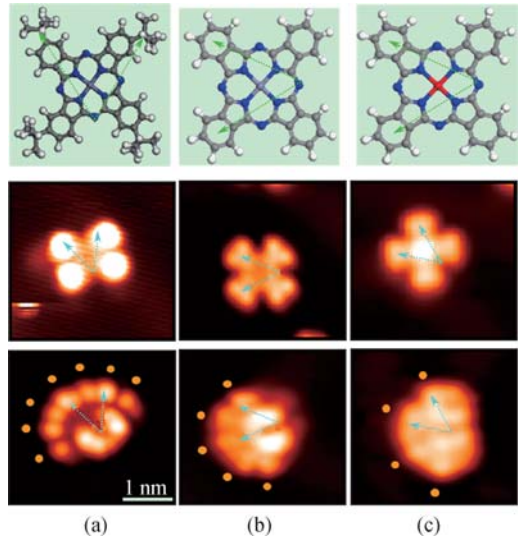

Fig. 7 Molecular structures and STM images showing molecular rotors formed by different molecules. (t-Bu)$_4$ZnPc **(a)**, ZnPc **(b)** and FePc **(c)**. They are all located at the elbow positions of the reconstructed Au(111) surface.

In addition to direct STM tip manipulation on the molecular position, the STM tunneling currents can also affect the rotation of molecular rotors. Figure 8 shows the current dependence of the (t-Bu)$_4$ZnPc molecular rotors. When increasing the tunneling current from a low current of 0.1 nA [Fig. 8(a)] to a higher one of 0.2 nA [Fig. 8(b)], the molecule rotates more actively so that the degree of circular of the rotation pattern becomes larger, which becomes more obvious when the current was kept for a period of time [Fig. 8(c)]. When the current is increased to 0.9 nA, a full circle of rotation pattern can be clearly observed [Fig. 8(d)]. This gradual increase in the degree of the circular arc means that the molecular rotation movement becomes more active and can gradually override the barrier formed by the Au(111) reconstruction and covers the whole circle eventually. The above result shows a gradual activation process while increasing the current. Since the molecular rotation can be driven

by thermal energy, the STM current provides another way driven by the rotation of the molecules.

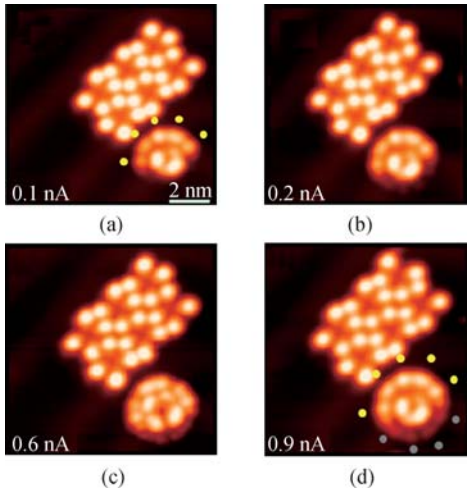

Fig. 8 A sequence of STM images showing tunneling current effect on the (t-Bu)$_4$ZnPc molecular rotor when the sample bias was kept at –1.3 V. Tunneling currents for each image are **(a)** 0.1 nA, **(b)** 0.2 nA, **(c)** 0.6 nA, **(d)** 0.9 nA, respectively. The molecular rotor can sweep faster and more degree ranges as the tunneling current increases.

4 Summary

Single molecular rotors self-assembled into ordered molecular rotor arrays by depositing (t-Bu)$_4$ZnPc on the Au(111) surface. The rotation of several metal phthalocyanine single molecules at reconstructed Au(111) surfaces has been realized. The different motion state of the molecular rotors can be tuned by depositing molecules on different regions of the reconstructed Au(111) surface or by changing the configurations of the molecules. The molecular rotors can be switched on or off with a STM tip. The rotating mechanism has been investigated by experiment and first-principle calculations. It was found that the gold adatom plays a vital role in the molecular rotors. It provides a rotation axis for the molecular rotor via the bond forming between gold adatom and the nitrogen atom in the molecule. The present results indicate that except for thermal, the intensity of tunneling current can also be used to control the rotation. It undoubtedly sheds new light on the application of single molecular rotors in the field of nano-scale devices.

Acknowledgements The authors would like to thank D. X. Shi, L. Gao, X. Lin, Z. H. Cheng, Z. T. Deng, N. Jiang, W. Ji, J. T. Sun, and Y. Y. Zhang for invaluable assistance in experiments and theoretical simulations. Work at IOP was partially supported by the NSFC, MOST and CAS in China.

References

1. J. V. Barth, G. Costantini, and K. Kern, Nature, 2005, 437: 671
2. J. V. Barth, Annu. Rev. Phys. Chem., 2007, 58: 375
3. A. R. Pease, J. O. Jeppesen, J. F. Stoddart, Y. Luo, C. P. Collier, and J. R. Heath, Acc. Chem. Res., 2001, 34: 433
4. A. Facchetti, M. H. Yoon, and T. J. Marks, Adv. Mater., 2005, 17, 1705
5. O. M. Yaghi, O. K. M, N. W. Ockwig, H. K. Chae, M. Eddaoudi, and J. Kim, Nature, 2003, 423: 705
6. Q. Liu, Y. Y. Zhang, N. Jiang, H. G. Zhang, L. Gao, S. X. Du, and H. J. Gao, Phys. Rev. Lett., 2010, 104: 166101
7. N. Jiang, Y. Y. Zhang, Q. Liu, Z. H. Cheng, Z. T. Deng, S. X. Du, H. J. Gao, M. J. Beck, and S. T. Pantelides, Nano Lett., 2010, 10: 1184
8. H. J. Gao and L. Gao, Prog. Surf. Sci., 2010, 85: 28
9. W. Ji, Z. Y. Lu, and H. Gao, Phys. Rev. Lett., 2007, 99 (5): 059602
10. L. Gao, W. Ji, Y. B. Hu, Z. H. Cheng, Z. T. Deng, Q. Liu, N. Jiang, X. Lin, W. Guo, S. X. Du, W. A. Hofer, X. C. Xie, and H. J. Gao, Phys. Rev. Lett., 2007, 99: 106402
11. M. Feng, L. Gao, S. X. Du, Z. T. Deng, Z. H. Cheng, W. Ji, D. Q. Zhang, X. F. Guo, X. Lin, L. F. Chi, D. B. Zhu, H. Fuchs, and H. J. Gao, Adv. Funct. Mater., 2007, 17: 770
12. D. Shi, W. Ji, X. Lin, X. He, J. Lian, L. Gao, J. Cai, H. Lin, S. Du, F. Lin, C. Seidel, L. Chi, W. Hofer, H. Fuchs, and H. J. Gao, Phys. Rev. Lett., 2006, 96: 226101
13. L. Gao, Z. T. Deng, W. Ji, X. Lin, Z. H. Cheng, X. B. He, D. X. Shi, and H. J. Gao, Phys. Rev. B, 2006, 73: 075424
14. M. Feng, X. F. Guo, X. Lin, X. B. He, W. Ji, S. X. Du, D. Q. Zhang, D. B. Zhu, and H. J. Gao, J. Am. Chem. Soc., 2005, 127: 15338
15. Y. L. Wang, W. Ji, D. X. Shi, S. X. Du, C. Seidel, Y. G. Ma, H. J. Gao, L. F. Chi, and H. Fuchs, Phys. Rev. B, 2004, 69: 075408
16. L. Gao, Q. Liu, Y. Y. Zhang, N. Jiang, H. G. Zhang, Z. H. Cheng, W. F. Qiu, S. X. Du, Y. Q. Liu, W. A. Hofer, and H. J. Gao, Phys. Rev. Lett., 2008, 101: 197209
17. G. S. Kottas, L. I. Clarke, D. Horinek, and J. Michl, Chem. Rev., 2005, 105: 1281
18. J. Vacek and J. Michl, Adv. Funct. Mater., 2007, 17: 730
19. D. Zhong, T. Blomker, K. Wedeking, L. Chi, G. Erker, and H. Fuchs, Nano Lett., 2009, 9: 4387
20. J. Vacek and J. Michl, Proc. Natl. Acad. Sci. USA, 2001, 98: 5481
21. P. Kral and H. R. Sadeghpour, Phys. Rev. B, 2002, 65: 161401
22. S. Tan, H. A. Lopez, C. W. Cai, and Y. Zhang, Nano Lett., 2004, 4: 1415
23. J. Berna, D. A. Leigh, M. Lubomska, S. M. Mendoza, E. M. Perez, P. Rudolf, G. Teobaldi, and F. Zerbetto, Nature Mater., 2005, 4: 704
24. K. Petr and S. J. Tamar, Chem. Phys., 2005, 123: 184702
25. J. E. Green, J. Wook Choi, A. Boukai, Y. Bunimovich, E. Johnston-Halperin, E. DeIonno, Y. Luo, B. A. Sheriff, K. Xu, Y. Shik Shin, H. R. Tseng, J. F. Stoddart, and J. R. Heath, Nature, 2007, 445: 414
26. T. R. Kelly, H. De Silva, and R. A. Silva, Nature, 1999, 401:

150
27. K. V. Mikkelsen and M. A. Ratner, Chem. Rev., 1987, 87: 113
28. P. Kral, Phys. Rev. B, 1997, 56: 7293
29. R. A. Van Delden, M. K. J. ter Wiel, M. M. Pollard, J. Vicario, N. Koumura, and B. L. Feringa, Nature, 2005, 437: 1337
30. G. London, G. T. Carroll, T. F. Landaluce, M. M. Pollard, P. Rudolf, and B. L. Feringa, Chem. Commun., 2009: 1712
31. C. Manzano, W. H. Soe, H. S. Wong, F. Ample, A. Gourdon, N. Chandrasekhar, and C. Joachim, Nature Mater., 2009, 8: 576
32. N. Henningsen, K. J. Franke, I. F. Torrente, G. Sehulze, B. Priewisch, K. Ruck-Braun, J. Dokic, T. Klamroth, P. Saalfrank, and J. I. J. Pascual, Phys. Chem. C, 2007, 111: 14843
33. B. C. Stipe, M. A. Rezaei, and W. Ho, Science, 1998, 279: 1907
34. A. Zhao, Q. Li, L. Chen, H. Xiang, W. Wang, S. Pan, B. Wang, X. Xiao, J. Yang, J. G. Hou, and Q. Zhu, Science, 2005, 309: 1542
35. P. Wahl, L. Diekhöer, G. Wittich, L. Vitali, M. A. Schneider, and K. Kern, Phys. Rev. Lett., 2005, 95: 166601
36. N. Tsukahara, K.-I. Noto, M. Ohara, S. Shiraki, N. Takagi, Y. Takata, J. Miyawaki, M. Taguchi, A. Chainani, S. Shin, and M. Kawai, Phys. Rev. Lett., 2009, 102: 167203
37. X. Chen, Y. S. Fu, S. H. Ji, T. Zhang, P. Cheng, X. C. Ma, X. L. Zou, W. H. Duan, J. F. Jia, and Q. K. Xue, Phys. Rev. Lett., 2008, 101: 197208
38. B. C. Stipe, M. A. Rezaei, and W. Ho, Science, 1998, 280: 1732
39. J. K. Gimzewski, C. Joachim, R. R. Schlittler, V. Langlais, H. Tang, and I. Johannsen, Science, 1998, 281: 531
40. B. C. Stipe, M. A. Rezaei, and W. Ho, Science, 1998, 279: 1907
41. J. K. Gimzewski and C. Joachim, Science, 1999, 283: 1683
42. J. A. Stroscio and D. M. Eigler, Science, 1991, 254: 1319
43. P. Avouris, Acc. Chem. Res., 1995, 28: 95
44. F. Rosei, M. Schunack, Y. Naitoh, P. Jiang, A. Gourdon, E. Laegsgaard, I. Stensgaard, C. Joachim, and F. Besenbacher, Prog. Surf. Sci., 2003, 71: 95
45. C. Joachim, J. K. Gimzewski, and A. Aviram, Nature, 2000, 408: 541
46. D. M. Eigler, C. P. Lutz, and W. E. Rudge, Nature, 1991, 352: 600
47. C. Wöll, S. Chiang, R. J. Wilson, and P. H. Lippel, Phys. Rev. B, 1989, 39: 7988
48. J. V. Barth, H. Brune, G. Ertl, and R. J. Behm, Phys. Rev. B, 1990, 42: 9307
49. M. Peter, C. S. Dan, and T. John Yates Jr., Phys. Rev. Lett., 2006, 97: 146103
50. L. Limot, J. Kröer, R. Berndt, A. Garcia-Lekue, and W. A. Hofer, Phys. Rev. Lett., 2005, 94: 126102
51. H. G. Zhang, J. H. Mao, Q. Liu, N. Jiang, H. T. Zhou, H. M. Guo, D. X. Shi, and H. J. Gao, Chin. Phys. B, 2010, 19: 018105